Vietnam Journal of Science and Technology ***62*** *(4) (2024) 931-941*

doi:10.15625/2525-2518/20157

Ag/Fe_3O_4 bifunctional nanocomposite for sers detection of non-steroidal anti-inflammation drug diclofenac

Duy Hai Bui[1], Do Chung Pham[2], Magdalena Osial[3], Marcin Pisarek[4], Anna Tycova[5], Thi Nam Pham[6], Thi Thanh Huong Nguyen[6], Thi Thu Vu[1, *], Thi Thanh Ngan Nguyen[1,*]

[1]*University of Science and Technology of Hanoi, Vietnam Academy of Science and Technology, 18 Hoang Quoc Viet, Cau Giay, Ha Noi, Viet Nam*

[2]*Hanoi National University of Education, 136 Xuan Thuy, Cau Giay, Ha Noi, Viet Nam*

[3]*Institute of Fundamental Technological Research, Polish Academy of Sciences, Pawińskiego 5B, 02-106 Warsaw, Poland*

[4]*Institute of Physical Chemistry, Polish Academy of Sciences, Kasprzaka 44/52, 01-224 Warsaw, Poland*

[5]*Institute of Analytical Chemistry, Czech Academy of Science, Veveří 97, 602 00 Brno, Czech Republic*

[6]*Institute of Tropical Technology, Vietnam Academy of Science and Technology, 18 Hoang Quoc Viet, Cau Giay, Ha Noi, Viet Nam*

[*]Emails: *nguyen-thi-thanh.ngan@usth.edu.vn; thuvu.edu86@gmail.com;*

Received: 19 February 2024; Accepted for publication: 23 May 2024

Abstract. In this work, a bifunctional nanocomposite based on silver and iron oxide nanoparticles ($AgNPs/Fe_3O_4$) was prepared by combining co-precipitation of Fe_3O_4 and in-situ reduction of AgNPs and then used as SERS (Surface-Enhanced Raman Scattering) substrate for sensing diclofenac which is one of the most widely used non-steroid anti-inflammation drugs. Morphology and structural studies revealed a conjugated structure in which silver nanoparticles (80 nm in diameter) were surrounded by iron oxide nanoparticles (18 nm in diameter). There is a slight blue-shift in position of plasmon peak from 405 nm for silver nanoparticles to 375 nm for $AgNPs/Fe_3O_4$ nanocomposite. Even the saturation magnetization (M_s) of the Ag/Fe_3O_4 nanocomposite only reached 28 $emu \cdot g^{-1}$ but still good enough for immobilizing nanocomposite structures onto the substrate. The detection limit and enhancement factor of the SERS-based diclofenac sensor were found to be 10^{-12} M and 2.6×10^{10}, respectively. Such kind of bifunctional nanocomposite will probably help us to avoid time-consuming process to immobilize metal nanoparticles onto the surface, and also allow us to regenerate the substrate for multiple uses.

Keywords: AgNPs, Fe_3O_4, bifunctional, SERS, NSAIDS.

Classification numbers: 2.2.1, 2.9.4, 3.2.1.

1. INTRODUCTION

The overdose of diclofenac (DCF), a common anti-inflammatory drug, may cause serious issues such as aplastic anemia, gastrointestinal disorders, and disturb in renal function [1]. For

the detection of DCF, many analytical approaches have been developed such as spectroscopy techniques, electrochemistry, enzyme-linked immunosorbent assay, chromatography techniques [2]. These approaches share common drawbacks such as slow performance, difficult sample preparation, costly equipment, excessive use of organic solvents. As a result, the development of low-cost devices with high accuracy for on-site analysis of DCF in water samples is urgently needed.

Recently, SERS (Surface-Enhanced Raman Scattering) sensors are gaining more attention in food safety and drug analysis [3]. Basically, the working principle of SERS sensor is based on the coupling between Raman (inelastic scattering of photons) and plasmon effects of metallic nanostructures. At close approximation nearby surface of metal nanostructures, the Raman fingerprint signals from targeted molecules can be enhanced up to 10^{14} times via resonance process. Some other advantages of SERS technique can be named as non-destructive measurement and good selectivity.

SERS sensors for DCF (also other NSAIDs) identification and detection have been developed recently by several research groups. In order to enable the regeneration of SERS substrates, one might combine plasmonic behavior of noble metallic nanoparticles and superparamagnetic behavior of iron oxide material. The two materials can be prepared either in core-shell structure (usually iron oxide core and silver shell) or in conjugated structure (one material is surrounded by the other one). In the former structure, the surface iron oxide nanoparticles are generally modified with the aid of silica ad-layer and suitable linking agents before coating with a thin shell layer of silver [4]. It must be noticed that this is a time-consuming process in which many expensive reagents are needed. In the later form, either silver nanoparticles will be grown onto the surface of iron oxide nanoparticles or the two materials can be grown together in one-pot approach. For instance, Z. Y. Bao *et al*. have reported the in-situ reduction of silver ions on the surface of iron oxide microspheres to generate Ag/Fe_3O_4 conjugated structure [5]. Another approach is to prepare Ag/Fe_3O_4 nanocomposite via one-pot procedure in which the two metallic precursors were added to reaction mixture so that the two materials can grow in the same time. The use of a 'sticky' reagent such as 4-mercaptobenzoic acid might improve the adsorption and order of Ag/Fe_3O_4 particles onto the substrate. Several biological reducing reagents (i.e, exine compounds from pollen grains) might be employed to offer a green way to prepare Ag/Fe_3O_4 nanocomposite. In some cases, the organic layer at middle region (i.e, polyacrylic acid) between silver and iron oxide materials might become an internal SERS reference to improve the reliability and enable quantification of analytes. It was reported that the conjugated structure of the hybrid nanocomposite might provide better enhancement factors compared to core-shell structures [6]. The bifunctional material Ag/Fe_3O_4 can be also utilized in other applications such as catalytic degradation of organic pollutants, antibacterial tests, and even energy storage [7].

Herein, we employ a conjugated structure with silver nanoparticles (NPs) surrounded by iron oxide nanoparticles ($AgNPs/Fe_3O_4$). The introduction of magnetic particles will surely facilitate the concentration of metal nanoparticles onto the substrate, and then easily removed them when needed. The iron oxide nanoparticles were first prepared via a co-precipitation process from iron salts in ammonia solution, and then silver nanoparticles were grown in an aqueous solution containing magnetic particles via a reduction process with the aid of hydroxylamine. The APTMS linker (3-aminopropyltrimethoxysilane) was additionally introduced to provide linkage between metal and oxide particles. The morphological and structural behaviors of the as-prepared nanocomposite will be carefully evaluated using scanning electron microscopy (SEM), Transmission electron microscopy (TEM), UV-vis spectrometry

(UV-vis), X-ray diffraction (XRD), X-ray photoelectron spectroscopy (XPS) techniques. The saturation magnetization of the material will be estimated from Vibrating Sample Magnetometer (VSM). The enhancement factor of Raman signals coming from targeted drug molecules will be calculated to evaluate the efficiency of the use of AgNPs/Fe_3O_4 composite as a substrate material.

2. EXPERIMENTS

2.1. Synthesis of Fe_3O_4 nanoparticles

By co-precipitating ferric and ferrous salts (from Beijing Chemicals Corporation, China) in the presence of argon gas, Fe_3O_4 magnetic nanoparticles were synthesized. 100 mL of deionized water was dissolved with 16.25 g $FeCl_3$ and 6.35 g $FeCl_2$. Chemical precipitation was obtained at 25 °C under vigorous stirring using magnetic stirrer by adding NH_4OH solution (29.6 %). The pH was maintained at around 10 throughout the procedure and the black precipitate was obtained. The color of the iron solution changes during the synthesis process from yellow to brown-black. The mixture solution was continuously stirred by a magnetic stirrer during this process. The precipitates were heated at 80 °C for 30 min, washed several times in water and ethanol after the synthesis, and then, dried in a vacuum oven at 70 °C.

2.2. Preparation of AgNPs/Fe_3O_4 nanocomposite structures

First, 0.05 g of Fe_3O_4 NPs was added to 100 mL of ethanol and sonicated for 30 min to facilitate binding with APTMS (3-aminopropyltrimethoxysilane 97 %), Sigma Aldrich). Then, 0.2 mL of APTMS was added, then vigorously agitated for 6 h. The particles were repeatedly washed in absolute ethanol after being removed from the solution by a magnetic field, and dried for 1.5 h in a vacuum oven at 70 °C. After that, AgNPs/Fe_3O_4 nanoparticles were formed by reducing $AgNO_3$ (> 99.8 %, Beijing Chemicals), with hydroxylamine hydrochloride while having Fe_3O_4 NPs that had been coated with APTMS. Briefly, 100 mL of a 0.15 wt.% $AgNO_3$ solution received 0.05 g of Fe_3O_4 before being sonicated for 30 min. 100 mL of freshly made reductant, which was a combination of 45 mL of 0.06 M hydroxylamine hydrochloride and 50 mL of 0.1 M NaOH solution, was added and stirred for an additional 45 min. The last particles were acquired by applying a magnetic field and washing them in water until the supernatant became transparent and obtained.

2.3. SERS detection of diclofenac

For the SERS measurement, 25 µL of AgNPs/Fe_3O_4 NPs in water were put on a glass slide placed on top of the magnet, then DCF 10^{-8} M solution was added on top of NPs droplets. After the substrates were dried under ambient conditions, five spectra were collected at different positions of the substrates and the average of these spectra was used as the final spectrum for the sample. To optimize the testing conditions, the SERS substrates were prepared with different concentrations but same volume of nanocomposite structures deposited on to the same substrate area. The concentrations of AgNPs/Fe_3O_4 nanoparticles were varied from 0.2 to 0.4 mg·mL^{-1}. The optimal concentration was then used to detect DCF with different concentrations to evaluate the sensitivity of nanocomposite AgNPs/Fe_3O_4-based SERS substrate. These measurements were carried out in HR Evolution Raman system at 1 % power of 532 nm laser.

3. RESULTS AND DISCUSSIONS

3.1. Morphology studies

The morphological behaviors of the samples were examined by capturing the scanning electronic microscopy (SEM, Hitachi -4800) and transmission electronic microscopy (TEM, Zeiss Libra 120 Plus, Stuttgart, Germany, operating at 120 kV) images (as shown in Figure 1). SEM image of AgNPs/Fe_3O_4 nanoparticles shows the formation of conjugated structure made of silver nanoparticles (80 nm) surrounding by iron oxide nanoparticles (15-20 nm). Due to the difference in electron scattering ability between the two materials, the AgNPs are found in darker region with higher contrast whereas Fe_3O_4 NPs are found in lighter region with lower contrast [6]. The spherical shape is commonly found in metal and magnetic particles prepared in similar conditions [8]. Meanwhile, it was also shown that iron oxide particles (particle size below 20 nm) were aggregated forming large clusters if silver is not incorporated into the particles. From TEM images, the average size of AgNPs/Fe_3O_4 nanoparticles were also estimated to be 80 nm and 18 nm, respectively. It is doubtless that the APTMS linker with one amine end and one silane end is the main contributor to the strong attachment between metal and oxide particles. Otherwise, the use of hydroxylamine as reducing agent during the growth of silver nanoparticles might have also helped to improve the adhesion between the two counterparts of this metal-oxide conjugation [4].

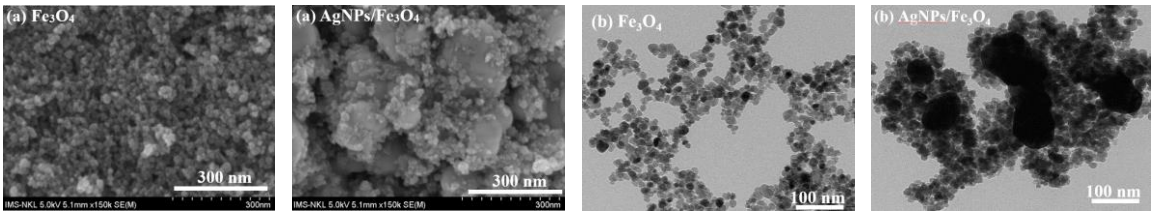

Figure 1. (a) SEM and (b) TEM images of Fe_3O_4 and AgNPs/Fe_3O_4.

Compared to core-shell structure as observed in other works, the proposed morphology of AgNPs/Fe_3O_4 composite shows several advantages as follows. First, since the magnetic particles are not fully covered by non-magnetic AgNPs, the magnetization of the composite is still sufficient to ensure an easy deposition/ removal of the complex onto/from the substrate using an external magnetic field. J. Ma *et al.* have reported that the AgNPs/Fe_3O_4 core-shell structure exhibits ferromagnetic behavior with the saturation magnetization less than 30 emu·g^{-1} even at the thickness of oxide coating up to 76 nm [4]. Second, the intrinsic aggregation of metal nanoparticles will surely be limited due to the presence of iron magnetic particles on their surface [9]. Lastly, the inter-particle distance between metal particles will also be kept close enough to ensure high efficiency of localized surface plasmon resonance due to the attraction between magnetic particles. These kinds of magnetic-plasmonic composite material are very suitable to be employed in microfluidic SERS systems (SERS sensors integrated onto microfluidic devices) whereas interfacial process are actually restricted.

3.2. Structural behaviors

3.2.1. XRD and EDX patterns

The X-ray diffraction (XRD, Bruker AXS D8 Advance) patterns of Fe_3O_4 and AgNPs/Fe_3O_4 nanocomposite structures were recorded from 2θ = 10° to 70° to confirm the

composition and crystalline structure of synthesized materials. XRD pattern of Fe_3O_4 sample (Figure 2a) shows six characteristic peaks for Fe_3O_4 including 2θ = 30.1°, 35.5°, 43.0°, 53.4°, 56.9° and 62.7°. These sharp diffraction peaks are attributed to the (220), (311), (400), (422), (511), and (440) planes and reveal to the face-centered cubic phase of synthesized Fe_3O_4 (JCPDS card 3-0863, magnetite) [10].

Due to the higher atomic number of Ag compared to Fe_3O_4 [11], the scattering ability of Ag is much stronger and resulting in the dominant of relative reflection intensity of Ag in AgNPs/Fe_3O_4 sample. The typical peaks for Ag are 2θ = 38.1°, 44.6°, 67.4° which can be assigned to the (111), (200), and (220) Bragg's reflections (JCPDS card no.04-0783). The average crystal size can be estimated from the peak width using Debye-Scherrer equation, $D = \frac{k\lambda}{\beta\, cos\theta}$, where k = 0.95 is Scherrer's constant, λ is the X-ray wavelength (1.54178Å), β is the full width at half maximum (FWHM), and θ is the Bragg diffraction angle. The crystal sizes of Fe_3O_4 and AgNPs/Fe_3O_4 nanocomposite NPs were calculated to be 18 nm and 92 nm, respectively. These results are in a quite good agreement with those obtained from SEM and TEM images.

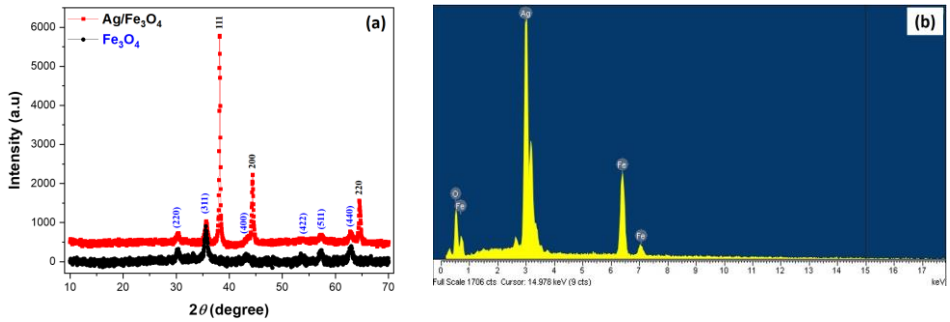

Figure 2. XRD patterns of Fe_3O_4 and AgNPs/Fe_3O_4 (a); EDX spectrum of AgNPs/Fe_3O_4 nanocomposite nanoparticles (b).

The elemental composition on the surface of the synthesized AgNPs/Fe_3O_4 sample was determined with energy-dispersive X-ray spectroscopy (EDX) measurement. EDX spectrum (Figure 2b) shown that the AgNPs/Fe_3O_4 nanocomposite is mainly composed of silver (Ag), iron (Fe) and oxygen (O) elements. The atomic percentages of silver, iron and oxygen were estimated to be 18.37 %, 15.30 % and 66.33 %, respectively. The Ag/Fe ratio was found to be 1.2 which is close to the expected ratio of precursors.

3.2.3. XPS spectra

XPS (PHI 5000 VersaProbe) survey spectra of Fe_3O_4 and AgNPs/Fe_3O_4 samples (Figure 3a) confirm the presence of Ag, Fe, O elements. Typical Cl and N impurities from the synthesis of the investigated materials are also visible. The high-resolution XPS spectra of both samples was also provided to determine the binding states of the detected elements. The results have clearly confirmed the conjugation between Ag^0 and Fe_3O_4 nanoparticles in the AgNPs/Fe_3O_4 nanocomposite (see Figure 3b, c, d). First, the high-resolution Ag3d spectrum of AgNPs/Fe_3O_4 nanocomposite exhibits the two energy binding levels with a gap of 6.0 eV at 368.3 eV (Ag $3d_{5/2}$) and 374.3 eV (Ag $3d_{3/2}$) which are featured for Ag^0 state but not Ag^+ ions [9]. Second, the Fe2p deconvoluted XPS spectrum of AgNPs/Fe_3O_4 sample shows the two main peaks at 710.6 eV (spin 3/2) and 724.2 eV (spin 1/2) are assigned to $Fe^{2+/3+}$ [12]. The next peaks above the energy of 712.5 eV may refer to Fe-organic metal compounds, including Fe-Cl bonds, which

may have been formed during the synthesis of the studied materials as a surface contaminations. The satellite peaks around 719.0 eV and 732.0 eV which are usually used as fingerprints to identify the magnetite phase of iron oxide (Fe_3O_4) were observed clearly in the sample. Moreover, the main position of the oxygen peak at 530.2 eV suggests the presence of oxide-metal bonds, in this case Fe-O [40]. Subsequent binding energies of oxygen which are clearly seen above 531.0 eV can be attributed to oxygen and carbon functional groups [13], which is consistent with our previous observations when analyzing the iron Fe2p peak.

A similar correlation can be observed for Fe_3O_4 as a reference sample. As a result of the deconvolution procedure, the characteristic bonds for Fe2p and O1s were determined, which can be assigned to the Fe_3O_4 oxide (Figure 3e and f). The obtained data are in good agreement with the literature data [14]. Nevertheless, a slight change in the position of the Fe2p peaks was observed, the peaks at 711.1 eV and 724.7 eV in Fe_3O_4 were shifted to smaller binding energies at 710.6 eV and 724.2 eV when silver was added to the nanocomposite. Probably, this may be due to the interaction of the plasmonic metal with the iron oxide nanoparticles.

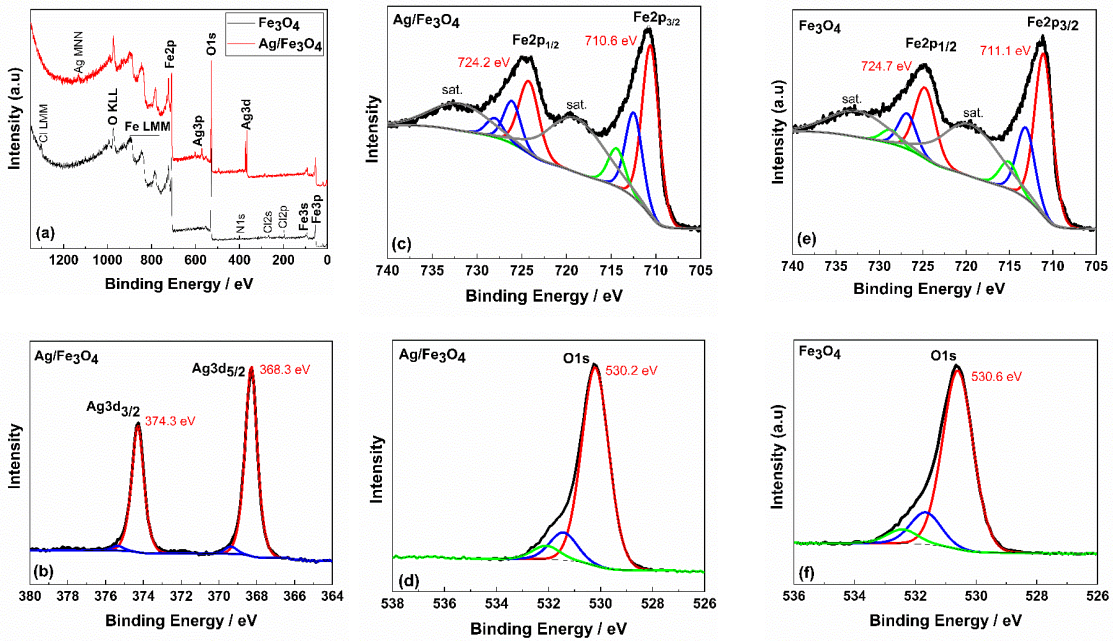

Figure 3. XPS spectra of Fe_3O_4 and AgNPs/Fe_3O_4 samples.

3.3. Surface plasmon resonance (SPR) behavior

The absorption spectra of the Ag, Fe_3O_4, and AgNPs/Fe_3O_4 samples recorded on JASCO V-730 UV-VIS Spectrophotometer are shown in Figure 4. The Fe_3O_4 sample shows a blear shoulder in the range from 350 nm to 400 nm, while the Ag sample exhibits a strong SPR peak centered at 405 nm. These results are in good agreement with previous reports [15, 16]. When the two materials (Fe_3O_4 and Ag) are combined in a composite, there is a blue-shift in the position of SPR peak from 405 nm (in AgNPs) to 375 nm (in AgNPs/Fe_3O_4). The position of plasmon absorption generally depends on several factors such as the particle size and shape, the intraparticle distance, and the medium. A red shift in plasmon peak (by 63 nm) was also previously observed in AgNPs/Fe_3O_4 composite due to the increase in particle size and reduction in inter-particle gap distance [5]. Oliveira-Filho *et al*. have shown a red shift in the position of

plasmon peak in Au@Fe_3O_4 core-shell structure (by 20 nm) due to the change in dielectric environment. Contrastly, R. Chhopra *et al.* have reported that the position of plasmon peak in Ag@Fe_3O_4 core-shell nanocluster was blue-shifted by 23 nm (compared to bare AgNPs). The absorption peak of AgNPs/Fe_3O_4 heterodimer was found to remain at the same position with that in AgNPs [6].

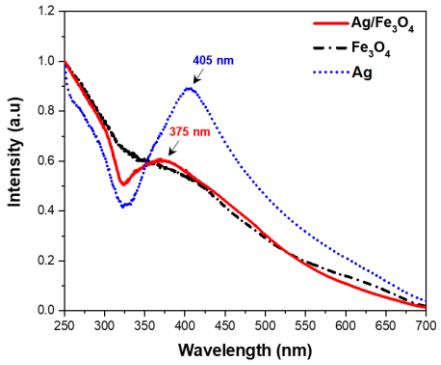

Figure 4. UV-vis spectra of Fe_3O_4 and AgNPs/Fe_3O_4 samples.

3.4. Magnetic analysis

Vibrating sample magnetometer (VSM) measurement was performed to evaluate magnetic behavior of the as-prepared samples. As seen in Figure 5, the magnetization curves of the samples show superparamagnetic properties of Fe_3O_4, i.e without hysteresis and remanence. The saturation magnetization (M_s) for Fe_3O_4 and AgNPs/Fe_3O_4 samples reaches values of 64 and 28 emu·g^{-1}, respectively. The silver nanoparticles with diamagnetic behavior and the non-magnetic linker APTMS may be responsible for this decrease in M_s value (43.75 %). It must be noted that only metal particles with the size less than 2 nm might exhibit paramagnetic or ferromagnetic behavior whereas metallic structures are generally diamagnetic. Since the size of silver nanoparticles is around 80 nm (as evidenced by SEM and TEM images), it is understandable that the saturation magnetization M_s of the composite material was significantly smaller compared with pure magnetic particles. In previous works, it was shown that the magnetization in AgNPs/Fe_3O_4 samples can be decreased by 40 % - 70 % [5, 6]. However, a moderate value of saturation magnetization is still sufficient for further immobilization of metal nanostructures onto substrates in SERS sensing applications.

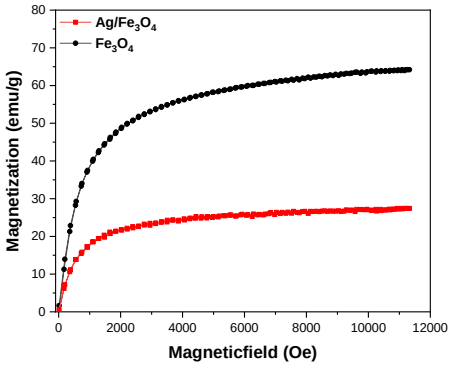

Figure 5. Magnetization curves of Fe_3O_4 and AgNPs/Fe_3O_4 samples.

3.5. SERS substrate based on AgNPs/Fe_3O_4 nanoscomposite for detection of diclofenac

It is essential to define the fingerprints of the samples in SERS sensors. In fact, the most characteristic band in the Raman spectrum of DCF which measured by Horiba LabRAM HR Evolution is triplet around 1600 cm^{-1} [15]. The bands at 1640 and 1610 cm^{-1} are given by the phenylacetate and dichlorophenyl ring stretching vibrations whereas the asymmetric carboxylate stretching vibration is located around 1560 cm^{-1}. Herein, the Raman shift relevant to asymmetric stretching vibration of the carboxylate (1560 cm^{-1}) was chosen as fingerprint of DCF on Raman spectra.

Firstly, we tested the amount of AgNPs/Fe_3O_4 nanocomposite to be deposited onto the substrate. A 25 µL drop of AgNPs/Fe_3O_4 suspension with concentration ranging from 0.2 to 0.4 mg·mL^{-1} was dropped on to the substrate, then left to be dried. A magnet was previously fixed under the substrate. The concentration of DCF was fixed to be 10^{-8} M. As seen in Figure 6, the Raman signals were decreased with increasing amount of nanocomposite and the highest signals were obtained at AgNPs/Fe_3O_4 nanocomposite concentration of 0.2 mg·mL^{-1} (Figure 6). Probably, the large amount of AgNPs/Fe_3O_4 nanocomposite has led to the formation of agglomerated clusters and then reduce the active plasmon surface area.

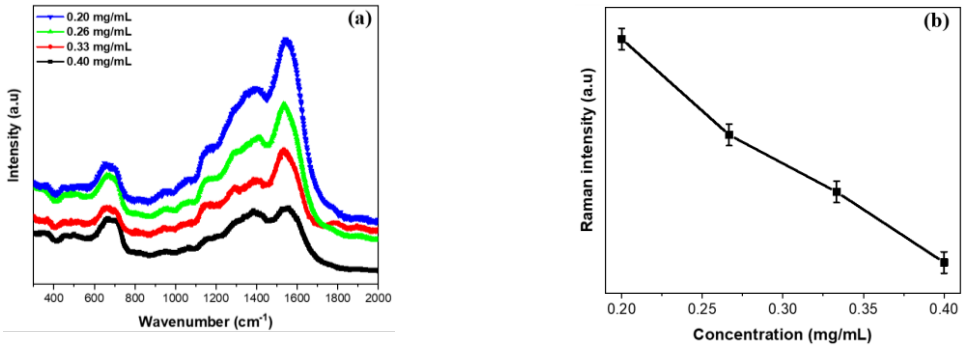

Figure 6. (a) The Raman spectra of DCF 10^{-8} M at different concentrations of AgNPs/Fe_3O_4 nanocomposite structures (0.2 mg mL^{-1}, 0.26 mg mL^{-1}, 0.33 mg mL^{-1}, 0.4 mg mL^{-1}), (b) A graph of Raman peak intensity at 1560 cm^{-1} and AgNPs/Fe_3O_4 nanocomposite concentration.

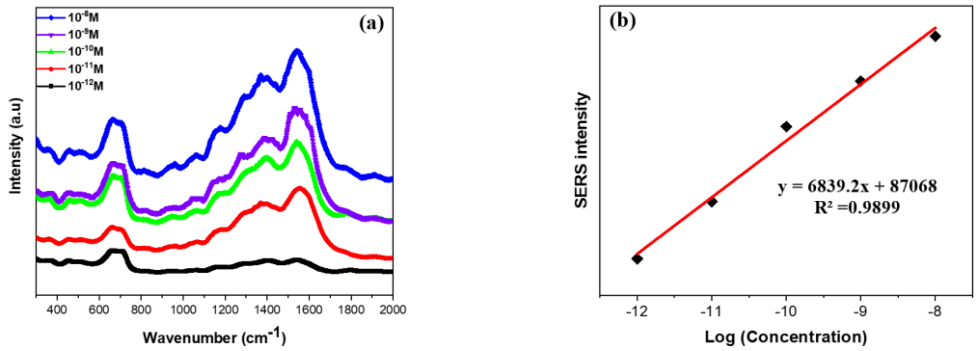

Figure 7. (a) SERS spectra of DCF with the concentrations ranging from 10^{-8} to 10^{-12} M and (b) intensity of DCF at 1560 cm^{-1} peak as a function of different concentrations in a logarithmic scale.

A calibration curve was then built with different DCF concentration ranging from 10^{-8} M to 10^{-12} M. The SERS substrate were prepared by drop-casting 25 µL of AgNPs/Fe_3O_4 NPs suspension (0.2 mg·mL^{-1}) and dried naturally at room temperature. The DCF solutions with

known concentrations were then dropped onto SERS substrates. The substrates were washed thoroughly with water to remove unbound DCF molecules. Of course, a magnet was always fixed under the substrate. As shown in Figure 7a, the Raman intensity at 1560 cm^{-1} increased with increasing sample concentration with the linear regression equation as follows:

$$I_{1560} = 6839.2* \log(C_{DCF}) + 87068 \ (R^2 = 0.989).$$

The limit of detection (LOD) is defined as the concentration of analyte at three standard deviations of the blank signal by the following:

$$\text{LOD} = 3.3 * \sigma/S$$

where 3.3 is the signal/noise ratio, σ is the standard deviation, and S is the slope of the calibration curve shown in Figure 7b, respectively. Herein, the LOD was determined to be 10^{-12} M. This value is quite low with those obtained in previous works [5, 16]. The enhancement factor (*EF*) is an essential parameter to evaluate the magnification of the Raman signal of targeted molecules interacting with the plasmonic nanostructures in SERS sensors. Under the same preparation conditions and identical experimental conditions (such as normalized of laser power, acquisition time, etc.), the SERS *EF* can be defined as:

$$EF = \left(\frac{I_{SERS}}{I_{NR}}\right)\left(\frac{C_{NR}}{C_{SERS}}\right)$$

where I_{SERS} stands for the SERS intensity in which DCF was counted at the peak 1560 cm^{-1} using AgNPs/Fe_3O_4 substrate. I_{NR} implies the normal Raman intensity of DCF at the same peak and without substrate. C_{NR} and C_{SERS} are the concentrations of DCF in the normal Raman experiment without substrate, and SERS experiment with substrate, respectively. In this study, the I_{SERS} was counted at 1560 cm^{-1} peak at the concentration of 10^{-12} M, and the I_{NR} was 1704.23 (1560 cm^{-1} peak) at the concentration of 10^{-2} M. The obtained enhancement factor is $EF = 2.6\times10^{10}$ which is superior compared to those obtained in previous works [16].

The great enhancement factor in sensing performance of SERS sensor based on AgNPs/Fe_3O_4 nanocomposite can be explained as follows. Since the silver nanoparticles are surrounded by iron oxide nanoparticles, they should have been gathered in a well-ordered manner at closer intra-particle distance on the substrate [5]. On the other hand, it may increase the density of hot spots which intensified the localized surface plasmon resonances [6]. Besides, the pure metallic nanoparticles can easily aggregate to from big clusters which generally narrowed the resonance band or weakened the measured signals [5].

The good reproducibility is vital for the practical applications of SERS sensors. To evaluate this parameter, the SERS intensities for the band vibration of DCF at 1560 cm^{-1} were collected from ten random spots. The relative standard deviation (RSD) value of SERS signals was 6.1%, suggesting the highly reproducible of SERS signals.

4. CONCLUSIONS

This work reported here combines the advantages of the highly enhanced SERS effect from AgNPs and the magnetic property offered by Fe_3O_4 NPs. The results showed a successful formation of AgNPs/Fe_3O_4 conjugates with the size of metal particle around 80 nm and the interparticle distance less than 20 nm. The intensity of the plasmon peak resulted from silver nanoparticles is relatively strong even though the position of the peak is slightly blue-shifted. The saturation magnetization is reasonable so that the conjugated nanostructure could be immediately and firmly assembled onto glass slides by an external magnet. The SERS substrate

based on AgNPs/Fe_3O_4 bifunctional nanocomposite is able to detect diclofenac with detection limit of 10^{-12} M and enhancement factor up to 10^{10}. In our future work, this bifunctional nanocomposite will be further employed to enable a facile and reversible immobilization of metallic nanostructures inside microfluidic devices onto which SERS detector is integrated and coupled with capillary electrophoresis separation.

Funding Declaration. This research was funded by Vietnam Academy of Science and Technology (QTCZ01.02/22-23).

CRediT authorship contribution statement. Duy Hai Bui, Do Chung Pham, Magdalena Osial, Marcin Pisarek, Thi Nam Pham, Thi Thanh Huong Nguyen: Data curation, Formal analysis. Anna Tycova: Methodology, Visualization. Thi Thu Vu: Writing review and editing. Thi Thanh Ngan Nguyen: Writing original draft, Writing review and editing.

Competing Interest declaration. The authors declare that they have no known competing financial interests or personal relationships that could have appeared to influence the work reported in this paper.

REFERENCES

1. Lonappan L., Brar S. K., Das R. K., Verma M., and Surampalli R. Y. - Diclofenac and its transformation products: Environmental occurrence and toxicity - A review, Environ. Int. **96** (2016) 127-138.
2. Nguyen T. D., Nguyen T. T. T., Nguyen V. H., Pham T. L., Pham T. Y. – Simultaneous determination of paracetamol and diclofenac in wastewater by high-performance liquid chrotomatography method, Vietnam Journal of Science and Technology **61** (4) (2023) 599-608.
3. Ando D., Miyazaki T., Yamamoto E., Koide T., and Izutsu K. - Chemical imaging analysis of active pharmaceutical ingredient in dissolving microneedle arrays by Raman spectroscopy, Drug Deliv. Transl. Res. **12** (2) (2022) 426-434.
4. Ma J., Wang K., Zhan M. - Growth Mechanism and Electrical and Magnetic Properties of Ag–Fe_3O_4 Core–Shell Nanowires, ACS Appl. Mater. Interfaces **7** (29) (2015) 16027-16039.
5. Bao Z. Y., Dai J., Lei D. Y., and Wu Y. - Maximizing surface-enhanced Raman scattering sensitivity of surfactant-free Ag-Fe_3O_4 nanocomposites through optimization of silver nanoparticle density and magnetic self-assembly, J. Appl. Physics **114** (2013) 124305.
6. Huang J., Sun Y., Huang S., Yu K., Zhao Q., Peng F., Yu H., Wang H., and Yang J. - Crystal engineering and SERS properties of Ag–Fe_3O_4 nanohybrids: from heterodimer to core–shell nanostructures, J. Mater. Chem. **21** (44) (2011) 17930-17937.
7. Çıplak Z., and Yıldız N. - Ag@Fe_3O_4 nanoparticles decorated NrGO nanocomposite for supercapacitor application, J Alloys and Compounds **941** (2023) 169024.
8. Żygieło M., Piotrowski P., Witkowski M., Cichowicz G., Szczytko J., and Królikowska A. - Reduced Self-Aggregation and Improved Stability of Silica-Coated Fe3O4/Ag SERS-Active Nanotags Functionalized With 2-Mercaptoethanesulfonate, Front. Chem. **9** (2021) 697595.
9. Du J. and Jing C. - Preparation of Thiol Modified Fe3O4 @Ag Magnetic SERS Probe for PAHs Detection and Identification, J. Phys. Chem. C **115** (36)(2011) 17829-17835.

10. Wang J., Meng G., Tao K., Feng M., Zhao X., Li Z., Xu H., Xia D., Lu J. R. - Immobilization of Lipases on Alkyl Silane Modified Magnetic Nanoparticles: Effect of Alkyl Chain Length on Enzyme Activity, PLoS One **7** (8) (2012) e43478.
11. Wang X. H., Liu H. L., Zhang W. X, Cheng W. Z., Liu X., Li X. M., Wu J. H. - Synthesis and characterization of polymer-coated AgZnO nanoparticles with enhanced photocatalytic activity, RSC Adv. **4** (83) (2014) 44011-44017.
12. Liu H. L., Wu J. H., Min J. H., Lee J. H., and Kim Y. K. - Monosized Core–Shell Fe_3O_4 (Fe)/Au Multifunctional Nanocrystals, J. Nanosci. Nanotechnol. **9** (2) (2009) 754-758.
13. Yamashia T., Hayes P. - Analysis of XPS spectra of Fe^{2+} and Fe^{3+} ions in oxide materials, Appl. Surf. Sci. **254** (2009) 2441-2449.
14. Anderson J. F., Kuhn M., Diebold U. - Epitaxially grown Fe_3O_4 thin films: An XPS study, Surface Science Spectra **4** (1996) 266.
15. Fini A., Cavallari C., and Ospitali F. - Diclofenac Salts. V. Examples of Polymorphism among Diclofenac Salts with Alkyl-hydroxy Amines Studied by DSC and HSM, Pharmaceutics **2** (2) (2010) 136-158.
16. Quan Y., Tang X. H., Shen W., Li P., Yang M., Huang X. J., Liu W. Q. - Sulfur Vacancies-Triggered High SERS Activity of Molybdenum Disulfide for Ultrasensitive Detection of Trace Diclofenac, Adv. Opt. Mater. **10** (23) (2022) 2201395.